RAPID COMMUNICATION

A double toroidal analyzer for scanning probe electron energy spectrometer*

Xu Chun-Kai(徐春凯)†, Zhang Pan-Ke(张盼科), Li Meng(郦 盟), and Chen Xiang-Jun(陈向军)

Hefei National Laboratory for Physical Science at Microscale and Department of Modern Physics, University of Science and Technology of China, Hefei 230026, *China*
Synergetic Innovation Center of Quantum Information and Quantum Physics, University of Science and Technology of China, Hefei 230026, *China*

(Received 26 February 2014; revised manuscript received 26 March 2014; published online 8 May 2014)

An ultra-high vacuum (UHV) compatible electron spectrometer employing a double toroidal analyzer has been developed. It is designed to be combined with a custom-made scanning tunneling microscope (STM) to study the spatially localized electron energy spectrum on a surface. A tip–sample system composed of a piezo-driven field-emission tungsten tip and a sample of highly ordered pyrolytic graphite (HOPG) is employed to test the performance of the spectrometer. Two-dimensional images of the energy-resolved and angle-dispersed electrons backscattered from the surface of HOPG are obtained, the performance is optimized and the spectrometer is calibrated. A complete electron energy loss spectrum covering the elastic peak to the secondary electron peaks for the HOPG surface, acquired at a tip voltage of −140 V and a sample current of 0.5 pA, is presented, demonstrating the viability of the spectrometer.

Keywords: double toroidal analyzer, scanning probe electron energy spectroscopy, electron energy loss spectroscopy, secondary electron emission spectroscopy

PACS: 34.80.−i, 07.50.Ls, 68.49.Jk **DOI:** 10.1088/1674-1056/23/7/073402

1. Introduction

The spatially localized spectroscopic information from a surface is always attractive to both physicists and chemists. When combined with electron energy loss spectroscopy (EELS), scanning transmission electron microscopy (STEM) is capable of mapping the spatial variation of surface plasmons at the nanoscale[1–5] and even identifying single atoms in nanostructures.[6–9] On the other hand, with the same idea as STEM-EELS, the combination of scanning tunneling microscopy (STM) with EELS – here called scanning probe electron energy spectroscopy (SPEES) – also has a spectrum imaging ability with sub-nanometer spatial resolution. However, early attempts to develop such an instrument encountered great difficulties,[10–14] mainly due to the strong electric field introduced by the tip bias, which greatly compresses the backscattered electrons and reduces the count rate.[15] Therefore, a novel electron energy analyzer with high detection efficiency is required.

Toroidal analyzers (TA), which are capable of parallel detections of energies and scattering angles of the charged particles (e.g., electrons) over a large range, have been developed in a variety of fields that have encountered the problem of low count rate.[16–22] The preliminary work of combining a TA with a scanning tip system in our laboratory demonstrated a capability for spatially-resolved spectroscopic measurement by the SPEES technique.[23,24] As a significant improvement, the double toroidal analyzer (DTA), formed by juxtaposing two toroidal-sector electrode pairs, has the advantage of achieving a flat focal surface and normal incidence of particles onto the detector surface. This makes the detection efficiency uniform if a planar microchannel-plate detector is used. Moreover, by replacing the complex exit lenses assembly of a normal TA with a pair of concave toroidal electrodes, the DTA improves the performance of the spectrometer and makes the calibration and optimization work much easier.[25–30] In this article, we report an ultra-high vacuum (UHV) compatible electron spectrometer employing the DTA for the SPEES instrument. The performance of the spectrometer is tested using a tip–sample system composed of a piezo-driven field-emission tungsten tip and a sample holder. The backscattered electrons from a highly ordered pyrolytic graphite (HOPG) surface are analyzed by the DTA, and the energy-resolved and angle-dispersed image of the electrons acquired by a two-dimensional position-sensitive detector (PSD) is obtained. The calibration and optimization of the analyzer are carried out, and a complete electron energy loss spectrum is presented, covering the elastic peak to the secondary electron peaks for the HOPG surface, which is acquired at a tip voltage of −140 V and a sample current of 0.5 pA.

*Project supported by the National Basic Research Program of China (Grant No. 2010CB923301) and the National Natural Science Foundation of China (Grant Nos. 11327404 and 11174268).

†Corresponding author. E-mail: xuck@ustc.edu.cn

© 2014 Chinese Physical Society and IOP Publishing Ltd

2. Instrument

The SPEES apparatus is a combination of STM and DTA. The three-dimensional view of the spectrometer is illustrated in Fig. 1(a), in which the DTA and its relative orientation with the STM are shown. Only half of a whole DTA is used in this spectrometer for the purpose of being combined with a custom-made STM.[31] The open side of the DTA is covered by a supporting plate, which is also used as a base board to mount the DTA. The fringe field of the open side is compensated by a series of concentric ring electrodes of gold film printed on the ceramic plates by lithography. The schematic diagram of the cross section containing the cylindrical axis and line A–A' is shown in Fig. 1(b). In the SPEES experiment, a negative voltage is applied to the STM tip, causing a field emission electron beam incident onto the sample surface. The electrons are backscattered and those moving in the plane parallel to the sample surface are collected, focused, and accelerated/decelerated to the pass energy of the DTA by a five-element entrance lens assembly. Each element of the lenses is a pair of ring electrodes, the cross section of which is also illustrated in Fig. 1(b). The electrons passing through the exit aperture of the lenses will enter the double toroidal deflector, which is the juxtaposition of a convex toroidal sector pair with a deflection angle of 180° and a concave toroidal sector pair with a deflection angle of 90°. This combination will achieve a nearly flat focal plane normal to the direction of electrons at the exit of the second concave toroidal sector. The cylindrical radius a and the spherical radius b are 70 mm and 50 mm, respectively, for each of the two sectors. The deflected electrons are dispersed at the exit of the DTA, where a two-dimensional PSD is placed to detect the outgoing positions of the electrons.

The entrance lenses and the deflection sectors are all made of aluminum alloy and mounted on the supporting plate made of nonmagnetic stainless steel. All the surfaces seen by the electrons are coated with gold. The manufacturing precision is about 0.1 mm, and the mounting accuracy is better than 0.1 mm, which is ensured by dowels made of the PEEK material. The PSD consists of two microchannel plates (MCPs) of 80 mm in diameter in a chevron configuration followed by a gear-type resistive anode (RA). However, the effective detection area of the RA used in this apparatus is not large enough to cover the whole exit area of the DTA, we have to sacrifice a small part of the detection azimuthal range, and place the RA eccentrically as shown in Fig. 2. Considering that the data acquired at the edge of the exit area will be discarded due to the fringe electric field effect, this arrangement will barely affect the detection efficiency of the DTA. The voltage supply and signal processing circuitry for the PSD is the same as that in our previous SPEES instrument, which has been reported elsewhere.[23]

The apparatus is mounted in a vacuum chamber made of nonmagnetic stainless steel, which is pumped to an ultra-high vacuum environment of 2.5×10^{-8} Pa by an ion pump. The whole vacuum chamber is covered by a double layer of μ-alloy to shield it from external magnetic fields.

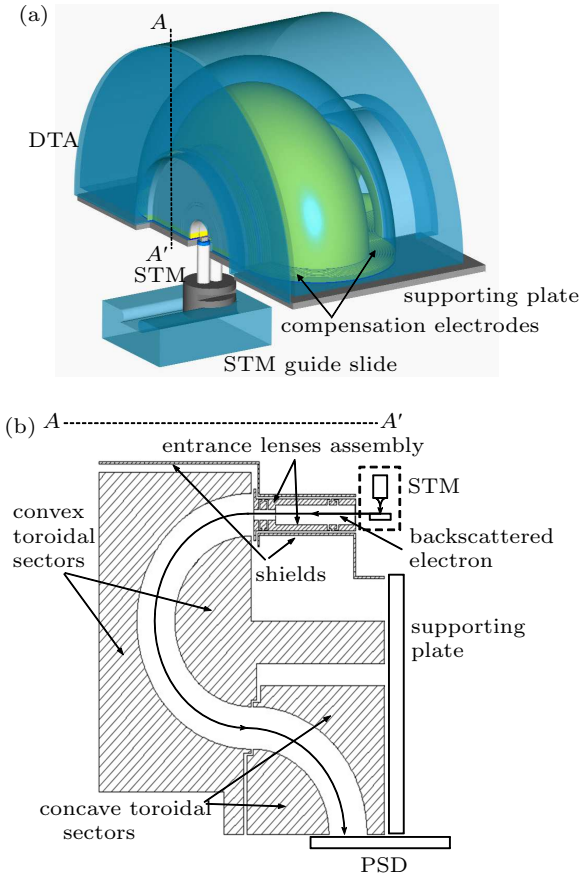


Fig. 1. (color online) (a) Three-dimensional view of the SPEES spectrometer. (b) Schematic diagram of the cross section containing the cylindrical axis and line A–A'.

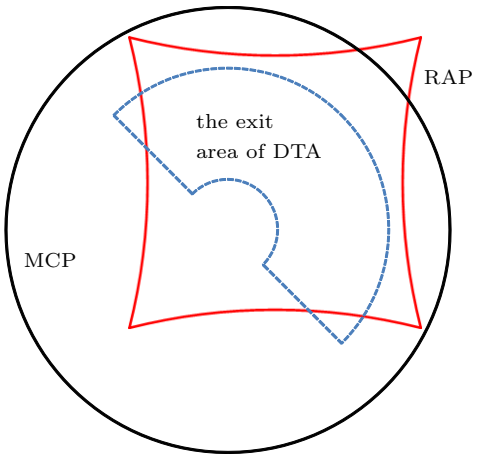


Fig. 2. (color online) Orientation of the RA relative to the MCP and the exit area of the DTA.

3. Experimental results

Experimental investigations have been carried out to study the electric optics and to optimize the performance of

the spectrometer. To do this, we employ a tip–sample system composed of a piezo tip driver and a sample holder. The tip is made from a tungsten wire by electrochemical etching, and the sample is HOPG, the clean surface of which is obtained by cleaving with an adhesive tape. During the experiment, a voltage of −140 V is applied to the tip, while the sample is grounded. The tip is driven to approach the sample surface until a sample current of several picoamps is detected. The elastically backscattered electrons from the HOPG surface are detected and used to test the spectrometer, and the change of the energy E of the electrons entering the DTA is realized by changing the voltage V_{L5} of the last element of the entrance lenses. The pass energy of the first pair of the toroidal sectors is set to be 100 eV, while that of the second pair is set to be 200 eV to improve the performance of the DTA.[29]

3.1. Calibrations and performance

Figure 3 shows one of the results of the calibration experiments. During the experiment, the voltage V_{L5} is scanned from −34 V to −50 V with an interval 2 V, therefore the energy of the electrons entering the DTA varies from 90 eV to 106 eV step by step. The image on the PSD is shown in Fig. 3(a), where a series of concentric arcs can be observed. The electrons with the same energy are supposed to impinge on the arc with the same radius on the PSD. Establishing a polar coordinate with its origin on the center of the arcs, the electron intensity distribution on radius r is calculated and shown in the inset of Fig. 3(a). By fitting this distribution with Gaussian functions, the peak position and the full width at half maximum (FWHM) of each peak can be obtained. The energy dispersion feature of the DTA is represented by the dependence of the electron energy E on its corresponding peak position, which is shown as solid squares in Fig. 3(b). The energy dispersion function is obtained by fitting these data with a quadric curve, which is shown as a solid line in the figure. By employing this function, the electron energy spectrum can be obtained by converting from the measured r-distribution spectrum, and the energy resolution can also be calculated. It is shown as opened circles in Fig. 3(b).

To optimize the performance of the DTA, the voltage applied to each element of the entrance lenses, denoted as V_{L1}, V_{L2}, V_{L3}, V_{L4}, and V_{L5} in order of the electron passing, is adjusted to optimize the performance of the DTA, which means better images of the concentric arcs and thereby better energy resolutions. Among these voltages, V_{L1} is kept grounded, and V_{L5} is determined by the incident electron energy and the pass energy of the first toroid. Therefore, three voltages are adjustable. Since it is impossible to test every combination of these three voltages, we just optimize them one by one based on numerical simulations. The final performance of the spectrometer is detailed in Table 1.

Table 1. The performance of the DTA.

Pass energy 1[a)]	Pass energy 2[b)]	Azimuthal range	Energy resolution	Energy window
100 eV	200 eV	85°	0.89 eV	16 eV

[a)] pass energy of the first pair of toroidal sectors;

[b)] pass energy of the second pair of toroidal sectors.

The performance of the DTA is mostly determined by the point to point focusing feature at a given pass energy. As can be seen in Fig. 3(b), the energy resolution remains almost unchanged in the energy range 92–104 eV, indicating that the point to point focal plane coincides with the PSD detection plane, and the resolution becomes poorer at 90 eV and 106 eV, which is apparently due to the fringe field effect. Compared with our previous SPEES instrument employing a TA,[23] this spectrometer achieves a better energy resolution at the same pass energy, better uniformity, and a wider energy window, which indicates that the incorporation of the DTA has surely improved the performance of the spectrometer.

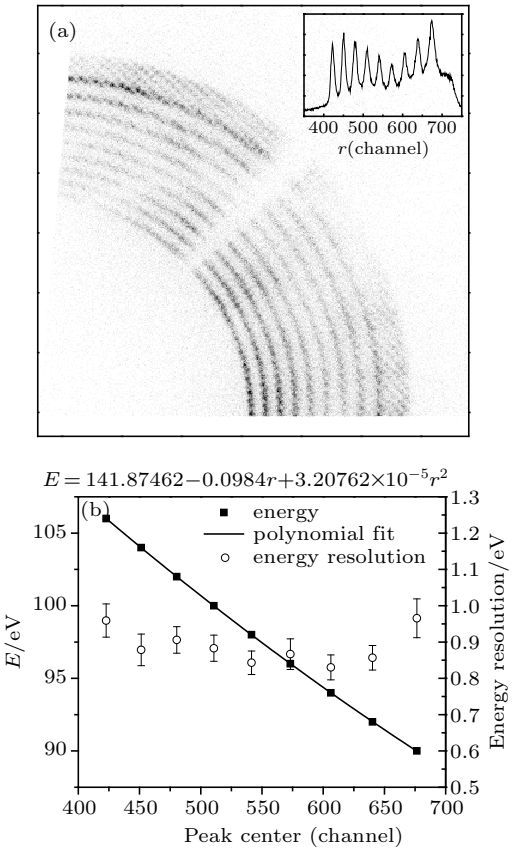


Fig. 3. Calibration of the spectrometer. (a) Two-dimensional image acquired by the PSD at the electron energies from 90 eV to 106 eV with an interval of 2 eV. The electron intensity distribution on radius r is shown in the inset. (b) The energy dispersion function and the energy resolution. See text for details.

Moreover, the apparatus is operated in an UHV environment, resulting in a very stable incident current field-emitted from the tip. Therefore, during the SPEES experiment, the scanning mode, which makes the detection energy range of

the DTA span the whole energy spectrum, can be employed to eliminate the non-uniform response of the PSD along the r coordinate.

3.2. Complete electron energy loss spectrum of HOPG

A complete electron energy loss spectrum of HOPG, covering the range from zero kinetic energy to zero loss (elastic) energy, is measured in scanning mode to test the performance of this DTA. The acquired spectrum is shown in Fig. 4(a), where we can see clearly both plasmon energy loss and secondary electron emission (SEE) features of the HOPG surface. The details of the spectrum at the low energy loss region (< 60 eV) is shown in the inset of Fig. 4(a), where two peaks due to the plasmon excitation of HOPG are observed. The low-energy-loss peak (~ 6 eV) is a π plasmon peak, which is assigned to the excitations involving the π electrons only, and the high-energy-loss peak (~ 22 eV) is a $\pi+\sigma$ plasmon peak, which is assigned to the excitations involving all the valence electrons (π and σ). On the other end of the spectrum, the SEE peaks of graphite are also observed, the detail of which is plotted against the kinetic energy, instead of the energy loss, in the range 0–60 eV in Fig. 4(b). At least five peaks (or shoulders) are observed in the SEE spectrum and are denoted as i–v by arrows. The assignments of the observed peaks based on the critical points in the theoretically calculated unoccupied band structure of graphite[32] are summarized in Table 2. The values are given relative to the Fermi level.

The measurement of the complete energy loss spectrum of HOPG indicates that this DTA can meet the requirements of SPEES experiments. After being combined with STM, further experiments on localized electron energy loss spectroscopy as well as secondary electron emission spectroscopy can be expected.

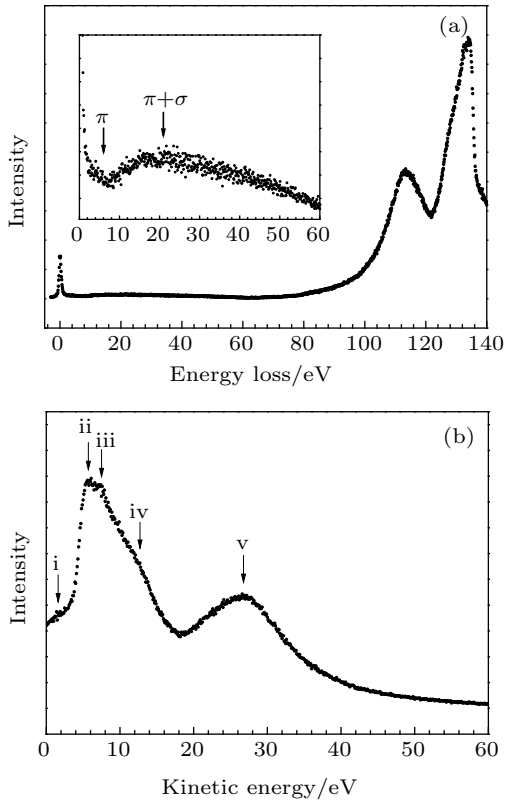


Fig. 4. (a) Complete electron energy loss spectrum of HOPG as obtained by the SPEES instrument. (b) Detail of the low-kinetic-energy region of the spectrum in panel (a).

Table 2. The assignment of the SEE peaks observed in Fig. 4(b).

Peak	Band assignment	Experimental/eV (in Fig. 4)	Theory/eV (Ref. [30])
i	$\pi(M_4^-)$	1.7	1.74(M_4^-)
ii	$\pi(\Lambda_2)$	5.7	6.04(Λ_2)
iii	$\sigma(\Gamma_1^+/\Gamma_6^-/M_1^+/M_2^-)$	7.4	7.35 (Γ_1^+/Γ_6^-)/7.30 (M_1^+)/7.45 (M_2^-)
iv	$\sigma(\Gamma_1^+/\Gamma_4^-)$	12.7	13.16 (Γ_1^+/Γ_4^-)
v	$\pi(M_4^-)$	27.0	27.19 (M_4^-)

4. Summary

In summary, we have developed a double toroidal analyzer (DTA), which is designed to be employed in an SPEES instrument. The calibration and the optimization have been carried out with a tip–sample system composed of a piezo-driven field-emission tungsten tip and a sample of cleaved HOPG surface, and the performance of the DTA has been tested. A complete electron energy loss spectrum of HOPG is acquired, which shows both energy loss features due to the plasmon excitation in the low energy loss region and the secondary electron emission features in the low kinetic energy region. This result indicates that this DTA is capable of fitting the SPEES instrument, and future work can be expected, combining it with STM.

References

[1] Bosman M, Keast V J, Watanabe M, Maaroof A I and Cortie M B 2007 *Nanotechnology* **18** 165505

[2] Nelayah J, Kociak M, Stéphan O, Abajo F J G, Tencé M, Henrard L, Taverna D, Pastoriza-Santos I, Liz-Marzán L M and Colliex C 2007 *Nat. Phys.* **3** 348

[3] Chu M W, Chen C H, García de Abajo F J, Deng J P and Mou C Y 2008 *Phys. Rev. B* **77** 245402

[4] Koh A L, Bao K, Khan I, Smith W E, Kothleitner G, Nordlander P, Maier S A and McComb D W 2009 *ACS Nano* **3** 3015

[5] Nicoletti O, Pena F, Leary R K, Holland D J, Ducati C and Midgley P A 2013 *Nature* **502** 80

[6] Suenaga K, Tencé M, Mory C, Colliex C, Kato H, Okazaki T, Shinohara H, Hirahara K, Bandow S and Iijima S 2000 *Scinece* **290** 2280

[7] Pennycook S J, Varela M, Lupini A R, Oxley M P and Chisholm M F 2009 *J. Electron Microsc.* **58** 87

[8] Suenaga K, Hasegawa K A, Niimi Y, Kobayashi H, Nakamura M, Liu Z, Sato Yuta, Koshino M and Iijima S 2012 *J. Electron Microsc.* **61** 285

[9] Zhou W, Oxley M P, Lupini A R, Krivanek O L, Pennycook S J and Idrobo J C 2012 *Microsc. Microanal.* **18** 1342

[10] Tomitori M, Hirade M, Suganuma Y and Arai T 2001 *Surf. Sci.* **493** 49

[11] Miyatake Y, Nagamura T, Hattori K, Kannemitsu Y and Daimon H 2003 *Jpn. J. Appl. Phys.* **42** 4848

[12] Palmer R E, Eves B J and Festy F 2002 *Surf. Sci.* **502** 224

[13] Festy F and Palmer R E 2004 *Appl. Phys. Lett.* **85** 5034

[14] Song M Y, Lawton J J, Robinson A P G and Palmer R E 2010 *Phys. Rev. B* **81** 161411

[15] Liu W J, Xu C K, Li Y G, Ding Z J, Xu K Z and Chen X J 2009 *Jpn. J. Appl. Phys.* **48** 122301

[16] Engelhardt H A, Black W, Menzel D and Liebl H 1981 *Rev. Sci. Instrum.* **52** 835

[17] Leckey R C G 1987 *J. Electron Spectrosc. Relat. Phenom.* **43** 183

[18] Huetz A, Lablanquie P, Andric L, Selles P and Mazeau J 1994 *J. Phys. B* **27** L13

[19] Reddish T J, Richmond G, Bagley G W, Wightman J P and Cvejanovic S 1997 *Rev. Sci. Instrum.* **68** 2685

[20] Berger D, Filippov M, Niedrig H, Rau E I and Schlichting F 1999 *J. Electron Spectrosc. Relat. Phenom.* **105** 119

[21] Siggel-King M R F, Lindsay R, Quinn F M, Pearson J, Fraser G and Thornton G 2004 *J. Electron Spectrosc. Relat. Phenom.* **137–140** 721

[22] Boeyen R W and Williams J F 2005 *Rev. Sci. Instrum.* **76** 063303

[23] Zhou X, Xu C K, Wei Z, Liu W J, Li J W, Chen X J, Williams J F and Xu K Z 2008 *J. Electron Spectrosc. Relat. Phenom.* **165** 15

[24] Xu C K, Chen X J, Zhou X, Wei Z, Liu W J, Li J W, Williams J F and Xu K Z 2009 *Rev. Sci. Instrum.* **80** 103705

[25] Toffoletto F, Leckey R C G and Riley J D 1985 *Nucl. Instrum. Methods Phys. Res. B* **12** 282

[26] Hellings G J A, Ottevanger H, Knibbeler C L C M, Engelshoven J and Brongersma H H 1989 *J. Electron Spectrosc. Relat. Phenom.* **49** 359

[27] Miron C, Simon M, Leclercq N and Morin P 1997 *Rev. Sci. Instrum.* **68** 3728

[28] Ren X G, Ning C G, Deng J K, Zhang S F, Su G L, Huang F and Li G Q 2005 *Rev. Sci. Instrum.* **76** 063103

[29] Lower J, Panajotovic R, Bellm S and Weigold E 2007 *Rev. Sci. Instrum.* **78** 111301

[30] Zhang P K, Xu C K, Tang Y G and Chen X J 2014 *J. Electron Spectrosc. Relat. Phenom.* **193** 39

[31] Hou Y B, Wang J H and Lu Q Y 2008 *Rev. Sci. Instrum.* **79** 113707

[32] Tatar R C and Rabii S 1982 *Phys. Rev. B* **25** 4126